

LThB4.pdf

Negative Feedback Avalanche Diodes as Single-Photon Solid State Photomultipliers at 1.5 μm

M. A. Itzler, X. Jiang, and K. Slomkowski

Princeton Lightwave Inc., 2555 US Route 130 South, Cranbury, NJ 08512 USA
 mitzler@princetonlightwave.com

Abstract: We present results for negative feedback avalanche diodes (NFADs), which are InP-based SWIR solid-state photomultipliers with single-photon sensitivity operated with just a DC bias. We demonstrate photon number resolution for a matrix of NFAD elements.

OCIS codes: (040.1345) Avalanche photodiodes; (040.5570) Quantum detectors; (030.5260) Photon counting

1. Introduction

From the perspective of performance, reliability, and cost, the most practical photodetector available today with single photon sensitivity between 1.0 and 1.6 μm is the InGaAs/InP single photon avalanche diode (SPAD). However, for general usage—especially free-running operation—even the best InP-based SPADs have constraints, including counting rate limitations, insensitivity to photon number, and complex external electronic circuitry to control arming and disarming of the device. The detrapping of carriers trapped during previous avalanches induces elevated dark count rates (DCR) if SPADs are re-armed too quickly, and these “afterpulsing” effects degrade DCR at high count rates. Additionally, although the macroscopic charge pulse response of a SPAD is quite useful for detecting single photons, these avalanches are generally only weakly dependent on the number of photons initiating the avalanche, and so they provide very little sensitivity to the number of simultaneously incident photons.

A fundamental shortcoming of conventional SPADs is the unchecked positive feedback inherent in their avalanche dynamics. To relieve some of the constraints on SPADs, we have monolithically integrated “negative feedback” elements with best-in-class SPAD structures to create negative feedback avalanche diodes (NFADs) with self-limiting avalanches exhibiting highly deterministic gain values. NFAD devices can provide dramatically smaller avalanches (e.g., $\sim 10^5$ carriers) with very tight avalanche charge distributions (i.e., charge excess noise $F(Q) < 1.1$). With smaller avalanche size, fewer carriers are trapped during each avalanche, thereby reducing “afterpulsing” effects. The NFAD design is also extremely simple to operate: with just a fixed dc bias voltage corresponding to the sum of the diode avalanche breakdown voltage V_b and the desired excess bias V_{ex} , the NFAD will autonomously execute the entire arm, avalanche, quench, and re-arm cycle associated with photon detection. Finally, with more deterministic gains providing lower charge excess noise, it also becomes possible to sum the signals from multiple NFADs on a single output channel to obtain photon number resolution. Such a “matrix” of NFAD active regions constitutes a solid-state equivalent of a microchannel plate photomultiplier tube (MCP-PMT). In this paper, we demonstrate the ability of a common-anode common-cathode 4 x 4 NFAD matrix to provide analog output signals exhibiting photon number resolution. This type of NFAD matrix promises to serve as an excellent pixel structure for next generation low-light-level imagers with single-photon sensitivity.

2. Negative feedback avalanche photodiode (NFAD) design

The underlying epitaxial structure of the NFAD is based on our state-of-the-art SPAD structure described elsewhere [1]. We introduce negative feedback using monolithic surface-integrated thin film resistors. This approach is conceptually equivalent to canonical passive quenching, in which avalanche current flow induces a voltage drop across a large external resistance and effectively removes this voltage from the diode, causing the avalanche to quench. Historically, though, hybrid integration has introduced large parasitic capacitance effects, and discharging and re-charging of these parasitic capacitances leads to large charge flow Q per avalanche. With monolithic integration, parasitic effects can be negligible, and the amount of charge flow Q required prior to avalanche quenching is determined by just the avalanche diode depletion capacitance C_d and the excess bias V_{ex} , i.e., $Q = C_d \times V_{ex}$. Ideally, each avalanche involves this same amount of charge flow Q , and Q can be made quite small through appropriate scaling of C_d . [The magnitude of the excess bias V_{ex} will be dictated by operational targets for photon detection efficiency (PDE) since PDE increases with larger V_{ex} .]

The choice of feedback resistance R_f is driven by a trade-off between quenching effectiveness and the re-arming time constant. A larger R_f provides more effective quenching since it will induce a larger voltage drop for a given value of instantaneous avalanche current; in fact, if R_f is too small, the avalanche will not quench at all [2] and a persistent current ensues. On the other hand, since the re-arming of the NFAD to the target excess bias V_{ex} requires the re-charging of C_d , the time constant for this re-arming is $R_f C_d$, and larger R_f leads to a longer re-arming process.

LThB4.pdf

3. NFAD avalanche statistics

We characterized the avalanche behavior of NFADs using a data acquisition board with 1-ns sampling resolution and deep memory allowing strings of data up to 250 ms long. The electrical interface to the device is a simple bias tee to provide DC applied voltage $V_a = V_b + V_{ex}$ and extract current pulses corresponding to avalanche events. A 20-dB transimpedance amplifier on the output provided signals of $\sim 10 - 100$ mV, depending on V_a . Figure 1(a) illustrates a number of avalanche pulses corresponding to dark counts during a 3- μ s period. An enlarged plot in Figure 1(b) of the pulse at 4280 ns shows that the full-width at half maximum of these pulses is about 2 ns.

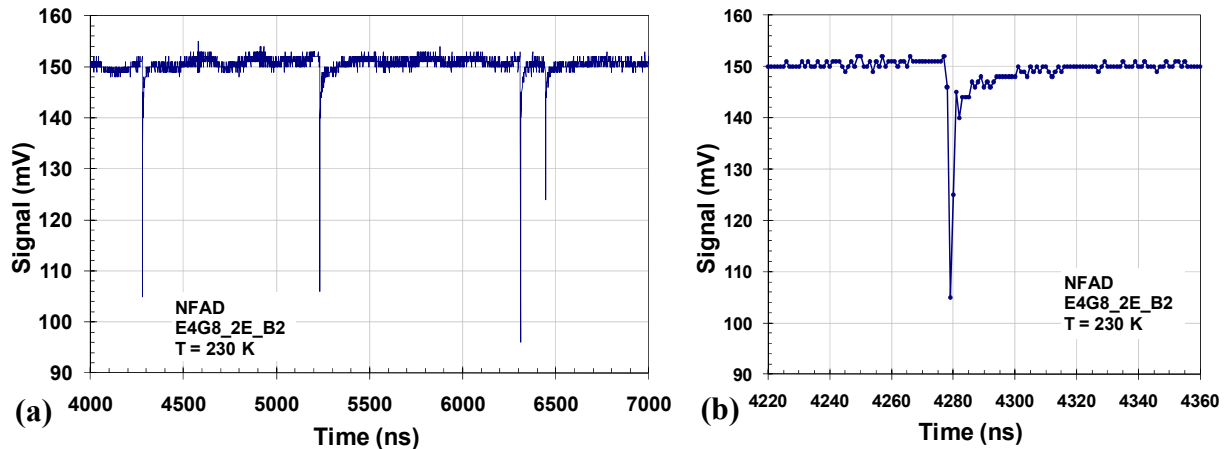


Fig. 1. (a) Pulse response from dark counts of NFAD device during 3 μ s period. (b) Enlargement of the first pulse from (a) at about 4280 ns, showing data points limited by the 1-ns time resolution of the measurements.

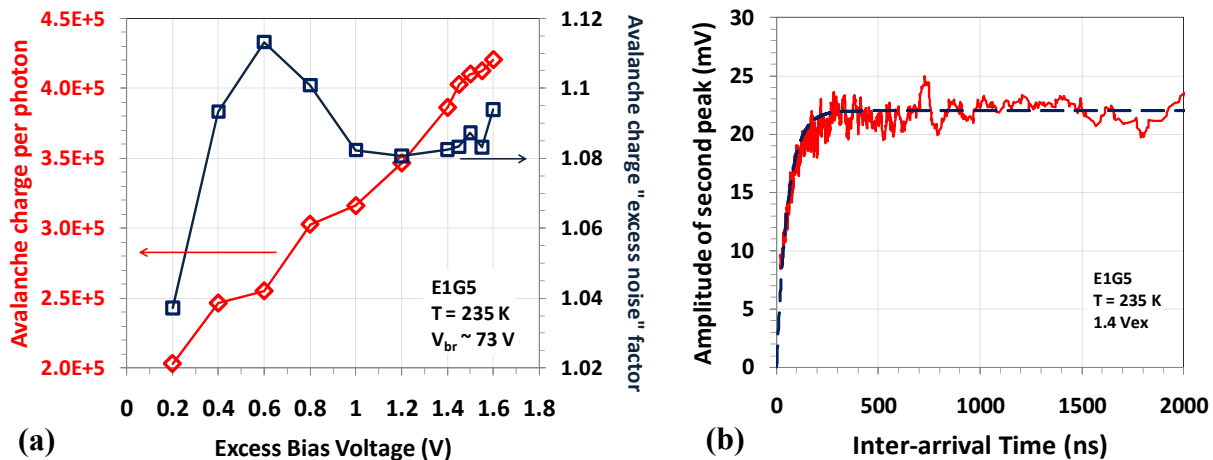


Fig. 2. (a) Measured avalanche charge per photon as a function of excess bias (red diamonds, left-hand axis) determined by integrating over pulse responses to incident photons. Fluctuations in the avalanche charge can be quantified by the charge "excess noise" $F(Q)$ (blue squares, right-hand axis); see text. (b) Exponential NFAD re-arming time constant can be extracted from consecutive pulse pair inter-arrival times, as described in the text.

In order to judge the uniformity of these pulses, we have carried out statistical analysis on both the peak height distribution as well as the total charge flow per pulse, as calculated by integrating over the current pulses. In Figure 2(a), we show avalanche charge statistics for avalanches induced by periodic single-photon arrivals. The average avalanche charge per photon varies in the range of $(2-4) \times 10^5$ e, depending on the bias voltage (red diamonds, left-hand axis). The variation in this avalanche charge at any given excess bias value can be expressed by a charge "excess noise" defined as $F(Q) = 1 + \sigma^2/\langle Q \rangle^2$ where $\langle Q \rangle$ is the average integrated charge and σ is the standard deviation of the distribution for Q . The dependence of $F(Q)$ on excess bias (blue squares, right-hand axis) shows that for excess bias values on the order of 1 V and larger, we find $F(Q)$ to be in the range of ~ 1.08 .

LThB4.pdf

Further insight can be obtained from the temporal separation between pairs of consecutive pulses and the dependence of the height of the second of these pulse pairs on their “inter-arrival time”. In particular, these data provide an effective method for determining the device re-arming time. The basic premise is that if two avalanche pulses occur with a very small temporal separation, the second pulse will be occurring with the device not fully re-armed, and the absolute height of this second pulse will be directly related to the extent of re-arming. The data in Figure 2(b) illustrates this behavior. The red curve, which is a moving average of the measured raw data, clearly shows the increase in second peak height with increasing inter-arrival time for short interarrival times (e.g., < 200 ns). The saturation of the second peak height at ~ 22 mV indicates full re-arming of the NFAD, and nearly full (~95%) re-arming—corresponding to 3 times the RC time constant for device re-charging—is achieved within about 165 ns. An exponential fit (in blue) to the measured data provides an exponential re-charging time constant $\tau \sim 55$ ns, which is in reasonably good agreement with an expected value of $\tau \sim 46$ ns based on estimates of $R_f C_d$.

4. NFAD matrix exhibiting photon number resolution for multi-photon pulses

The independent quenching and re-arming of NFAD devices allows for multiplexed configurations in which multiple devices connected in parallel can supply additive signals to a single pair of input/output interconnection traces. The micrograph on the right side of Figure 3 shows the front-side wiring of a 4×4 matrix of NFADs in such a configuration. By repeatedly illuminating this matrix with multi-photon optical pulses (from the back side of the chip), we obtain the distribution of avalanche sizes (measured in e^-) shown on the left side of Figure 3. To simulate this distribution, we consider that the charge excess noise $F(Q)$ found in Figure 2(a) was ~ 1.08 , which corresponds to a standard deviation for single avalanches given by $\sigma / \langle Q \rangle = 0.28$. We find an accurate fit to the data for a mean number of detected photons per optical pulse of $\eta = 2.9$, which is consistent with the optical power used after considering the present geometric fill factor of ~25% and the single active area detection efficiency of ~6% for the excess bias used. (Note that neither the measured data set nor the simulation include statistics for “zero-photon” pulses.) While this device does not yet provide highly resolved distributions of photon number—this will require a reduction in $F(Q)$ by further suppression of avalanche variations—the data does show that it can provide quasi-analog output similar to an MCP-PMT for multi-photon inputs. With appropriate size reduction, this device also has excellent prospects as the pixel structure of next-generation low-light-level imagers.

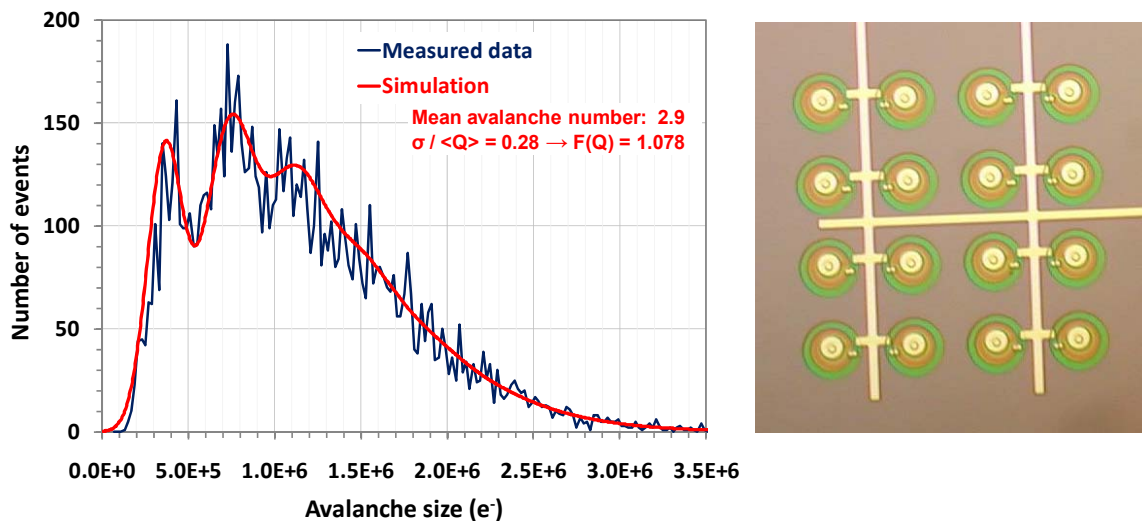


Fig. 3. Left: Measured distribution of avalanche sizes (blue curve) from a 4×4 NFAD matrix. Simulated distribution (red curve) for mean avalanche number $\eta = 2.9$ and avalanche charge excess noise of $F(Q) \sim 1.08$ provides a good fit to measured data. Right: Micrograph of 4×4 NFAD array showing common-anode electrical connections; each circular active area is $22 \mu\text{m}$ in diameter.

References

- [1] M. A. Itzler, X. Jiang, M. Entwistle, K. Slomkowski, M. Owens, A. Tosi, F. Acerbi, F. Zappa, and S. Cova, “Advances in InGaAsP-based avalanche diode single photon detectors,” *J. Modern Optics* **58**, Nos. 3–4, 174–200 (2011).
- [2] M. A. Itzler, X. Jiang, B. Nyman, K. Slomkowski, “InP-based Negative Feedback Avalanche Diodes,” *Proceedings of the SPIE* **7222**, 72221K (2009).